

Short-Term Solar Power Forecasting Based on CEEMDAN and Kernel Extreme Learning Machine

Ali Riza Gun^{1,*}, Emrah Dokur¹, Ugur Yuzgec², Mehmet Kurban¹

¹Department of Electrical Electronics Engineering, Bilecik S. E. University,
11210 Bilecik, Turkey

²Department of Computer Engineering, Bilecik S. E. University,
11210 Bilecik, Turkey

*aliriza.gun@bilecik.edu.tr, emrah.dokur@bilecik.edu.tr, ugur.yuzgec@bilecik.edu.tr,
mehmet.kurban@bilecik.edu.tr

Abstract—The use of renewable energy sources contributes to environmental awareness and sustainable development policy. The inexhaustible and nonpolluting nature of solar energy has attracted worldwide attention. Accurate forecasting of solar power is vital for the reliability and stability of power systems. However, the effect of the intermittency nature of solar radiation makes the development of accurate prediction models challenging. This paper presents a hybrid model based on Kernel Extreme Learning Machine (Kernel-ELM) and Complete Ensemble Empirical Mode Decomposition with Adaptive Noise (CEEMDAN) for short-term solar power forecasting. The decomposition technique increases the number of stable, stationary, and regular patterns of the original signals. Each decomposed signal is fed into Kernel-ELM. To validate the performance of the hybrid model, solar power data from the BSEU Renewable Energy Laboratory, measured at 5-minute intervals, are used. To validate the proposed model, its performance is compared to some state-of-the-art forecasting models with seasonal data. The results highlight the good performance of the proposed hybrid model compared to other classical algorithms according to the metrics.

Index Terms—Decomposition; Energy; Forecast; Hybrid method; Solar energy.

I. INTRODUCTION

The share of renewable energy sources in production is increasing rapidly, although most of the load demand of power systems is provided by conventional generation plants with limited resources and CO_2 emissions. Global warming, pollution, energy crises, and economic policies have made the use of renewable energy sources popular today. The low maintenance cost and natural availability of solar radiation have significantly increased the share of solar power generation systems among renewable energy sources [1]. While the installed power capacity of grid-connected solar power plants around the world has reached 707.495 MW by the end of 2020, China is the leader in this field with its installed power capacity of 253.834 MW [2]. In addition, Turkey aimed to increase the share of solar

power plants in installed power to the level of 300 GW, according to its 2023 targets [3]. Today, parallel to this rapid increase in installed power capacity, the integration of solar energy systems into power systems has brought with it the necessity of estimating the power to be obtained from these energy systems with precision accuracy. In various fields such as energy markets, grid management systems, reliability and stability of power systems; it is of great importance to estimate the energy to be obtained from intermittent and chaotic renewable energy sources such as wind and solar with high accuracy.

Researches are carried out in this field for four different time horizons: very short, short, medium, and long term. Although short-term forecasting is important in decision-making for power system operation, medium- and long-term forecasts are made for maintenance and planning. In terms of energy storage control and electricity market management, very short-term forecasting approaches come to the fore [4].

In the literature, solar power forecasting approaches are examined under two main headings: physical and statistical methods. Physical methods include wind, solar radiation temperature, pressure, etc. These methods are generally more reliable for long-term forecasting. On the basis of this methodology, it combines meteorological data and equations from atmosphere models to make forecasts. The disadvantage of the model is that inaccurate forecasts may occur when there are sudden changes in the values of meteorological variables. The statistical model is divided into two groups: Artificial Intelligence (AI) models and time-series models. By measuring the difference between the actual measured value of photovoltaic (PV) output in the past and its forecast value, these models reduce the inaccuracy. Due to this reason, the utilisation of artificial AI-based approaches with historical PV data has gained significant popularity in this field. The use of some methods such as Deep Feed Forward Networks (DFFNs) [5], Support Vector Machines (SVMs) [6], [7], Extreme Learning Machine (ELM) [8], [9], Multilayer Perceptron (MLP) [10], [11], Radial Basis Neural Network (RBFNN) [12], [13], etc.

provide success in estimating nonstationary time-series data accurately. Today, it is seen that hybrid AI approaches are very popular in this field. In addition to the use of hybrid models created with metaheuristic approaches, there are also methods performed with decomposition methods. Wavelet Transform-Partial Swarm Optimization-SVM (WT-PSO-SVM) [14], Genetic Algorithm-SVM (GA-SVM) [15], PSO-ELM [9] have been proposed by researchers as metaheuristic methods for solar power forecasting in hybrid approaches.

In recent studies, hybrid approaches using different nonlinear signal decomposition methods for solar power forecasting have become popular. In recent years, decomposition models have been used in hybrid approaches such as Complete Ensemble Empirical Mode Decomposition with Adaptive Noise-Long Short-Term Memory (CEEMDAN-LSTM) [16], Maximum Overlap Discrete Wavelet Transform-Seasonal Autoregressive Integrated Moving Average-Random Vector Functional Link (MODWT-SARIMA-RVF [17], Swarm Decomposition Feed Forward Neural Network (SWD-FNNN) [18]. Sahu, Shaw, Nayak, and Shashikant [1] in 2021 presents the use of decomposition models in the future work proposal and also shows the still popularity of studies in this field. While hybrid methods studies are discussed that compare different Empirical Mode Decomposition (EMD)-based approaches, there are also some limited studies comparing these decomposition methods with Swarm Decomposition (SWD) [19].

The main focus of this paper is to present an improved hybrid methodology based on the CEEMDAN decomposition technique and Kernel-ELM for solar power forecasting. The model is mainly composed of two parts:

1. CEEMDAN is proposed to decompose the original solar power time-series preprocessing. The decomposition step provides a more stationary and linear signal. The components of the signals obtained from various frequencies are modelled individually. As such, the forecasting performance is improved.
2. The preprocessed data are sent to the established Kernel-ELM forecasting model. Here, the short-term solar power prediction engine is used on the ELM network, which has a basic structure and a fast learning speed. Moreover, to obtain more stable and effective results for solar data, the radial basis kernel function is used in the ELM forecast model. The improved hybrid model is compared with some state-of-the-art models, including the EMD-MLP, SWD-MLP, LSTM, and single Kernel-ELM model. To validate all models' performance, real solar power data set is obtained from BSEU Renewable Energy Laboratory. Some statistical performance metrics are used to compare the models.

This paper is organised as follows. The decomposition method and the Kernel-ELM structure are explained in Section II. Section III presents the characteristics of the dataset in the BSEU Renewable Energy Laboratory and the performance metrics that will be used in the study. The results of the hybrid model performance analysis are presented in Section IV. Finally, the conclusions of the

article are explained in Section V.

II. MATERIAL AND METHODS

A. Complete Ensemble Empirical Mode Decomposition

An algorithm called "Complete Ensemble Empirical Mode Decomposition Adaptive Noise" (CEEMDAN) has become very popular in signal processing. To reduce the mode mixing problem, adaptive white noise is added to improve the decomposition performance. CEEMDAN is performed for time-frequency analysis and processing of nonlinear and nonstationary signals [20]. Signal wave patterns with different characteristics can be extracted using CEEMDAN and Intrinsic Mode Functions (IMFs) are obtained with different time scales with more stationary features [20].

The process of the CEEMDAN algorithm is given as below.

Step 1: White noise $V^i(t)$ is added to the original signal $S(t)$. It is represented as $S^i(t)$, $S^i(t) = S(t) + V^i(t)$, $i = 1, 2, \dots, I$. The experimental signal of EMD is decomposed to obtain $S^i(t)$, IMF_1 accordingly, i.e.,

$$IMF_1 = \frac{1}{I} \sum IMF_1^i, \quad (1)$$

$$r_1(t) = S(t) - IMF_1. \quad (2)$$

Step 2: Add white noise $V^i(t)$ to residue $r_1(t)$, pretend experiment i times ($i = 1, 2, \dots, I$) and each iteration includes EMD to extract $r_1^i = x(t) + V^i(t)$ to get the first-order component IMF_1^i .

Step 3: Step 2 is performed until the residual and IMF components have decreased to the point where EMD cannot no longer separate them. At the end of the process, the decomposed signal, $S(t)$, can be determined as follows [20]

$$S(t) = \sum_{i=1}^n IMF_i + r_n(t). \quad (3)$$

The iteration continues with the mirror expansion algorithm, the post-cycle details of which follow the same scheme as traditional EMD are shared in [21].

B. Kernel-based Extreme Learning Machine

The Extreme Learning Machine (ELM) is a learning technique that selects hidden nodes at random and analytically calculates the output weights of Single-hidden Layer Feedforward Neural Networks (SLFNs), as illustrated in Fig. 1. The ELM has the advantage that the input weights and biases are generated randomly and the hidden layer settings do not need to be tuned. Thus, ELM may easily achieve good generalisation performance at extremely fast learning speeds [22].

Input connection weights (ω_{ij}), biases (b_k), and connection weights (θ_k) are parameters of an SLFNN shown in Fig. 1. In the ELM algorithm, values of ω_{ij} and b_k and the number of hidden layer neurons (N_h) are randomly determined. Analytically, the following transactions are used to obtain the connection weight (θ_k) parameters.

Depending on the input and connection, the SLFNN output is determined as follows [22]

$$y_i = \sum_{j=1}^{N_h} \theta_j \phi(x_i \omega_j + b_j). \quad (4)$$

N number equations can be obtained since (4) has N training samples. The H matrix vector notation for these equations is as follows

$$H = \begin{bmatrix} \phi(x_1 \omega_1 + b_1) & \cdots & \phi(x_1 \omega_{N_h} + b_{N_h}) \\ \vdots & \vdots & \vdots \\ \phi(x_N \omega_1 + b_1) & \cdots & \phi(x_N \omega_{N_h} + b_{N_h}) \end{bmatrix}_{N \times N_h}. \quad (5)$$

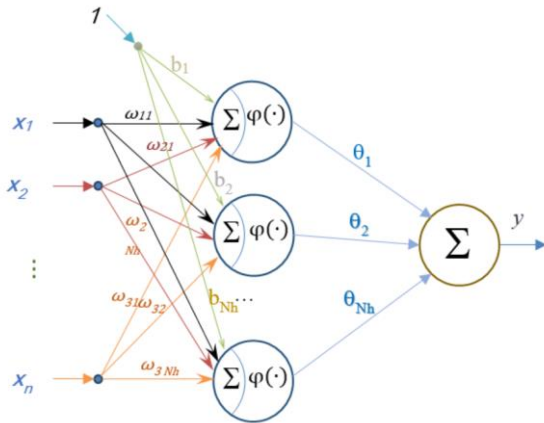


Fig. 1. Structure of the SLFNN model.

The target for each output, as well as its weights, are provided by

$$\begin{cases} T = H\gamma, \\ T = \begin{bmatrix} t_1 \\ \vdots \\ t_N \end{bmatrix}, \\ \gamma = \begin{bmatrix} \theta_1 \\ \vdots \\ \theta_{N_h} \end{bmatrix}. \end{cases} \quad (6)$$

By obtaining the inverse of the Moore-Penrose H matrix, the output connection weights are estimated [23]

$$\hat{\gamma} = H^+ T. \quad (7)$$

With this approach, the ELM often achieves a strong generalisation and a fast learning rate. The output weight can be calculated by adding a positive number $1/\lambda$ according to the orthogonal projection method and the ridge regression theory [24]

$$\hat{\gamma} = H^T \left(\frac{1}{\lambda} + HH^T \right)^{-1} T. \quad (8)$$

The ELM's output function is

$$y = h(x)\hat{\gamma} = h(x)H^T \left(\frac{1}{\lambda} + HH^T \right)^{-1} T. \quad (9)$$

Kernel-ELM was proposed by Huang [25]. A kernel matrix for ELM can be established in the event that the user is unaware of the feature mapping H. The following can be used to write (9).

The hidden layer feature mapping $h(x)$ does not need to be known in (10)

$$y = h(x)H^T \left(\frac{1}{\lambda} + HH^T \right)^{-1} T = \begin{bmatrix} k(x, x_1) \\ k(x, x_2) \\ \vdots \\ k(x, x_n) \end{bmatrix}^T \left(\frac{1}{\lambda} + HH^T \right)^{-1} T. \quad (10)$$

The user provides the kernel $k(u, v)$ that assumes the role of $h(x)$ and hidden nodes. The penalty factor is λ . The random mapping of the ELM is replaced by a stable kernel function, which improves the stability of the output weight. As a result, the Kernel-ELM is more generalisable than the ELM.

III. CASE STUDY

In terms of validation and test of the models, data from the Renewable Energy Laboratory at BSEU were used in the study. In addition to the characteristic of the data, this section also includes different performance metrics to show the accuracy of the model estimation.

A. Data Collection

To evaluate the performance of solar forecasting models, 5 minutes of actual production data from the BSEU Renewable Energy Laboratory (Fig. 2) in Bilecik, Turkey, for the period from January 2021 to September 2021, were used. Figure 2 shows the laboratory structure (Fig. 2(a)), battery systems (Fig. 2(b)), and 20 kW inverter Huawei Sun 2000 20 KTL (Fig. 2(c)). Table I presents information on the PV system. Data were collected in real time from the 20 kW inverter located in the output of the PV panel, by monitoring online. Although there are 63 polycrystalline solar panels with a total power of 190 W, in this study, a total of 36 panels containing 4 arrays, each with 9 panels, were commissioned. Each panel has an inclination angle of 40° and is located at 40.19°N , 29.96°E . Data are collected between 00:00 am and 23:55 pm, and although there are data points for each day, the values at the moment of the active power value obtained from the output of the inverter were recorded as 5 minutes. The recording process of the data received through the system established in November 2020, has started as of January 2021, and a total of 39.062 data have been monitored in real time and recorded on the Web to date. Table I presents the system information and the summary of the data.

The total data are 39.062, of which 70 % (27.343 data) are reserved for training and 30 % (11.719 data) are divided for testing. All models are run 50 times with the training and test sets, and the average error performance criterion of all studies is finally taken as the estimation accuracy.

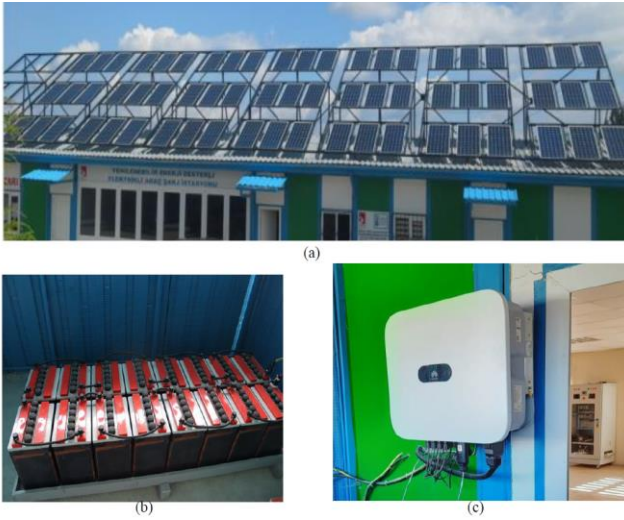


Fig. 2. BSEU Renewable Energy Lab: (a) Rooftop Solar PV; (b) Battery Systems; (c) Inverter.

Figure 3 shows data for all seasons from January 2021 to September 2021 for each 5-minute time horizon. Within the scope of the study, the one-month data for each seasonal sample were analysed separately and the comparative results are presented in Section IV.

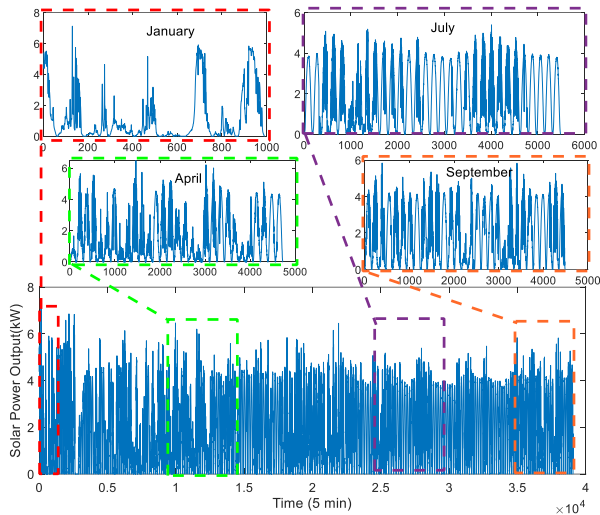


Fig. 3. The data set monitored for the 5-minute time horizon between January 2021 and September 2021.

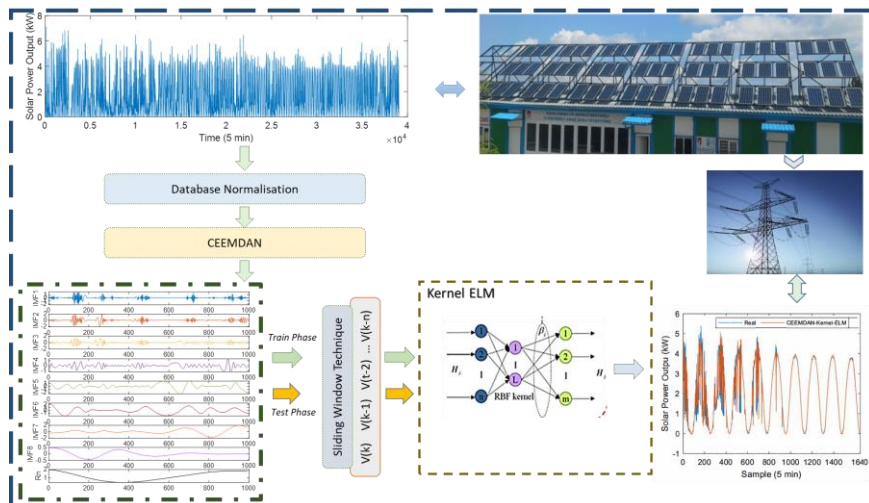


Fig. 4. Flow chart of the study.

TABLE I. PV SYSTEM AND DATA SUMMARY.

| | |
|---------------------|--------------------|
| Location | Bilecik, Turkey |
| Coordinates | 40.19 °N, 29.96 °E |
| Recorded data | Active power |
| Data resolution | 5 min |
| Number of PV panels | 36 |
| Capacity | 12 kWp |

B. Performance Metrics

The deviation of the predicted value from the target value in the test data set is taken into account while evaluating the performance of all models. To achieve this, in this paper, the Root Mean Square Error (RMSE), the Mean Square Error (MSE), and the Mean Absolute Error (MAE) metrics were used to verify the performance of the models. These metrics are shown in (11)–(13) [26]:

$$RMSE = \sqrt{\frac{\sum_{i=1}^N (y_i - \tilde{y}_i)^2}{N}}, \quad (11)$$

$$MSE = \frac{\sum_{i=1}^N (y_i - \tilde{y}_i)^2}{N}, \quad (12)$$

$$MAE = \frac{1}{N} \sum_{i=1}^N |y_i - \tilde{y}_i|. \quad (13)$$

Here y_i and \tilde{y}_i represent actual and predicted values, respectively. N is the total number of data used for performance evaluation and comparison. The MAE is the mean absolute forecast error of the forecast results. The physical basis for using RMSE/MAE is that it expresses the overall error for solar power forecasting for the entire test set.

IV. SIMULATION RESULTS AND DISCUSSION

In this section, the forecasting results of all implemented models, namely CEEMDAN-Kernel-ELM, SWD-MLP, EMD-MLP, single Kernel-ELM, and LSTM are discussed in detail. The original time-series of the months with sample data sets from each season presented in Fig. 3 were used in the analysis. To show the performance of the models in different characteristics, the results were carried out for one-month periods of each season. The study flow chart is presented in Fig. 4.

Hybrid methods were applied over three different modules, namely decomposition, forecasting, and combining. The original solar energy data normalised in the decomposition phase are separated into its subcomponents in this step by different decomposition methods. In the forecasting phase, separate MLP and Kernel-ELM models are created for each decomposed signal, and estimation is applied. All the results obtained here are collected in the last step and the output of the hybrid model is obtained. The decomposed signals of a sample month (July) are decomposed using the CEEMDAN method in seasonal analyses presented in Fig. 5. Here, the highest frequency component of the signal is indicated by IMF 1, while IMF 11 indicates the lowest frequency signal and the residual signal Rn . The decomposition results show that each signal exhibits unique qualities that point to various natural oscillation modes embedded in the series.

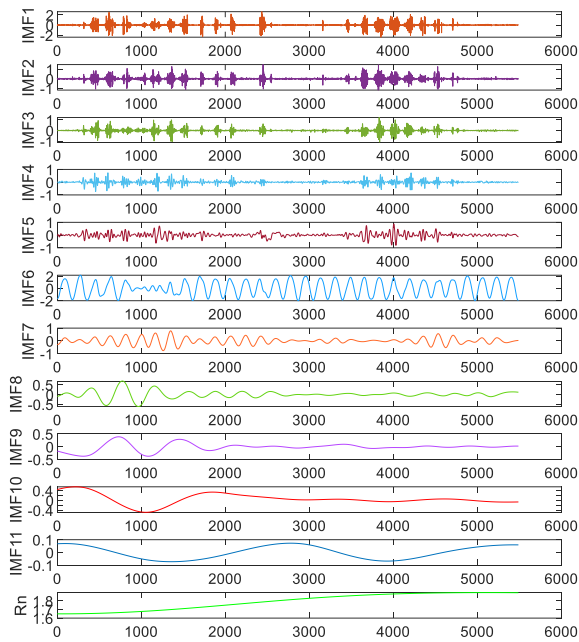


Fig. 5. CEEMDAN-based decomposition of the solar PV July time-series.

To the best of our knowledge, a swarm intelligent approach to the analysis of nonstationary signals, called “swarm decomposition”, has been applied for the first time to solar data for comparison with EMD-based models. Although it was used in [18] for the SWD solar power forecasting in 2020, attention was drawn to the importance of hybrid use rather than the superiority of this approach over other decomposition models. For this purpose, in this study, the SWD proposed by Apostolidis and Hadjileontiadis [27] for biomedical signals was used for comparison.

The data for September decomposed by the SWD algorithm are presented in Fig. 6. Since the prediction accuracy of the highest frequency component is predicted to be low, a second separation or elimination process can be applied for this signal. However, since the purpose of the study was to compare all separation methods with the same conditions in the study, no elimination or secondary separation process was applied. Separate MLP models were created for all subcomponents obtained after the

decomposition step. Here, using the sliding-window technique, the current value of the data and two steps before the MLP input were estimated after one step.

To compare the performance of the CEEMDAN-Kernel-ELM, the LSTM and single Kernel-ELM models are also used in the analysis. The aim of comparing the proposed model with LSTM is to show superiority of well-known deep learning approach. The LSTM has been especially used in time-series analysis in recent years. In this study, the number of hidden layers in the LSTM model was implemented for solar data by 2. The number of LSTM units required for four layers is calculated as 100, 100, 75, 75. A batch size of 16 and a maximum number of training epochs of 100 are chosen. The LSTM model implemented uses the Adam optimiser [45]. The learning rate is 0.005. Given that the model parameters are random, all LSTM models were tested 1001 times to reduce errors. Moreover, to show the superiority of hybrid models, a single Kernel-ELM model is added to the analysis.

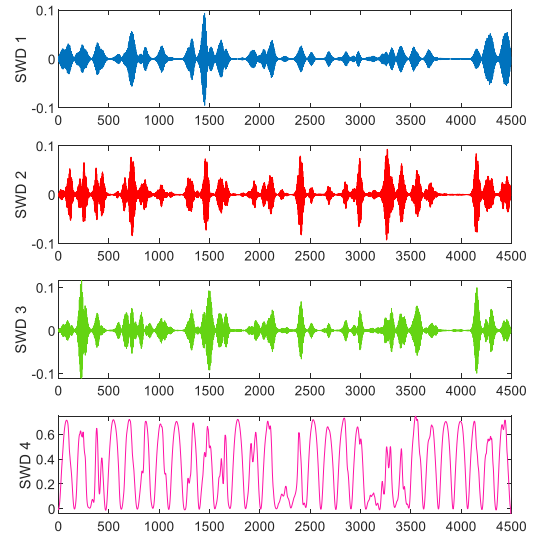


Fig. 6. SWD-based decomposition of solar PV September time-series.

The comparative test result of all models for July is presented in Fig. 7. A few of the prediction outcomes are depicted in figures for easier comprehension in this paper. Furthermore, Table II compares the solar power forecast results for the 5 min time horizon for the four months of January, April, July, and September using data from the BSEU Renewable Energy Laboratory.

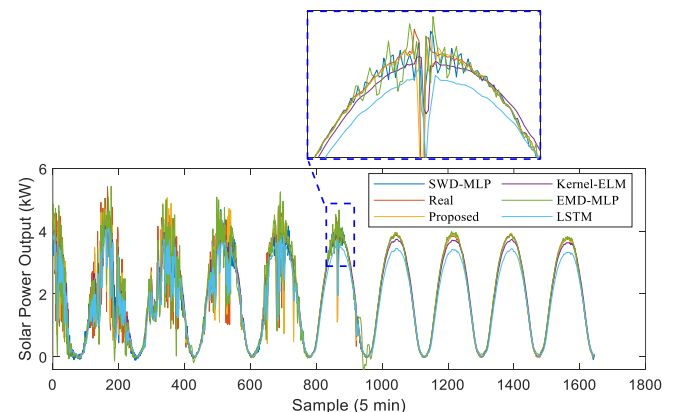


Fig. 7. Forecasting the test results for the July time-series.

TABLE II. COMPARATIVE ANALYSIS OF FORECASTING RESULTS FOR SOLAR POWER DATASETS.

| Months | Methods | RMSE | MSE | MAE |
|-----------|------------|--------|--------|--------|
| January | EMD-MLP | 0.3792 | 0.1438 | 0.2252 |
| | SWD-MLP | 0.4489 | 0.2015 | 0.2977 |
| | Kernel-ELM | 0.5902 | 0.3484 | 0.3741 |
| | LSTM | 0.6102 | 0.3723 | 0.3301 |
| | Proposed | 0.2546 | 0.1245 | 0.1870 |
| April | EMD-MLP | 0.2651 | 0.0703 | 0.1319 |
| | SWD-MLP | 0.3283 | 0.1078 | 0.2054 |
| | Kernel-ELM | 0.3317 | 0.1100 | 0.1777 |
| | LSTM | 0.3409 | 0.1162 | 0.2024 |
| | Proposed | 0.1820 | 0.0331 | 0.1226 |
| July | EMD-MLP | 0.3638 | 0.1324 | 0.1894 |
| | SWD-MLP | 0.4635 | 0.2148 | 0.2204 |
| | Kernel-ELM | 0.6372 | 0.4060 | 0.3974 |
| | LSTM | 0.5832 | 0.3401 | 0.2983 |
| | Proposed | 0.3460 | 0.1197 | 0.1396 |
| September | EMD-MLP | 1.2688 | 1.6098 | 0.4835 |
| | SWD-MLP | 0.5318 | 0.2828 | 0.2681 |
| | Kernel-ELM | 0.7096 | 0.5035 | 0.4551 |
| | LSTM | 0.6707 | 0.4499 | 0.3443 |
| | Proposed | 0.4111 | 0.1690 | 0.2217 |

As shown in the table, the RMSE, MSE and MAE error performance metrics of the proposed hybrid model (CEEMDAN-Kernel-ELM) for January were found to be 0.2546, 0.1245 and 0.1870, respectively, and it was concluded that the model performance was better than the other models. Although the EMD-MLP approach shows competitive results to the CEEMDAN-Kernel-ELM hybrid model, the proposed model has better accuracy according to all months. In particular, considering the month of September, it can be seen that the proposed model has a much lower error value.

Specifically, the proposed method reduced the RMSE performance error metric by 67.59 % compared to the EMD-MLP model in September. While SWD-MLP is a hybrid model, the standalone Kernel-ELM shows similar performance metrics for some months, such as April. It is seen that LSTM has the lowest model performance considering January, April, and July. Here, the hyper-parameters are selected the same for all LSTM models. To improve the model performance of the LSTM, it may be trained by some different parameters. However, this paper focused on the hybrid Kernel-ELM method, which is a faster model, rather than improving the LSTM model. According to the data shown in Table II, CEEMDAN-Kernel-ELM outperforms all other prediction models, with RMSE, MSE, and MAE metrics that are the lowest, compared to prediction models like EMD-MLP, SWD-MLP, standalone Kernel-ELM, and LSTM.

To describe the relationship between standard deviation, Root Mean Square Deviation (RMSD), and correlation coefficient, this paper uses the Taylor diagram presented in Fig. 8.

According to the results in Fig. 8, the closer the correlation coefficient value is to 1, the more linear the relationship between the actual data and the predicted data. However, the lower the standard deviation and RMSD values on the graph, the higher the performance of the model. According to Fig. 8, the CEEMDAN-Kernel-ELM model, which is represented by a black triangle, offers the best estimation result.

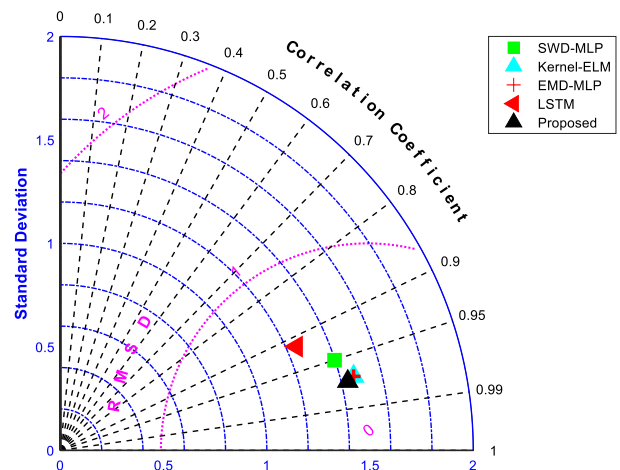


Fig. 8. Taylor diagram of the forecasting models of solar data.

As a result, the overall performance capability of the proposed hybrid model gave the best results monthly. It is a clear indication that the CEEMDAN-Kernel-ELM hybrid model can be accepted as a better data modelling tool for solar energy forecasting. Although the superiority of the SWD-MLP model was expected in this study, overall higher accuracy rates were achieved in the EMD-based models. This shows us the situation in which the optimal model cannot be selected for each decomposed signal. The MLP architectures are taken as the same, considering that it would be appropriate to make comparisons over the same values. If the model performance of the SWD-MLP model changes the architecture, it is likely to yield more competitive results.

V. CONCLUSIONS

In this study, an improved methodology based on the CEEMDAN and Kernel-ELM model is presented for solar power forecasting. The hybrid model combines the preprocessing step with CEEMDAN and the RBF kernel function. The decomposition step improves the performance of the model because of the acquisition of more linear and stable data. The kernel function process enables ELM eliminated tuning of hidden layer random weights and biases. Using performance metrics such as RMSE, MSE, and MAE, the prediction accuracy of the various prediction models is verified. Through the simulation results of the data collected from the BSEU Renewable Energy Laboratory, the CEEMDAN-Kernel-ELM model has significantly improved solar power forecast accuracy compared with the other four methods (EMD-MLP, SWD-MLP, Kernel-ELM, and LSTM). It is further verified that the forecasting results of the proposed hybrid model are better than the results of the single model. The proposed method reduced the MAE performance error metric by 50 % as compared to the Kernel-ELM model in January. Considering the all months, the comparison results indicate that the proposed CEEMDAN-Kernel-ELM outperforms other models for all the cases with the lowest error metrics values. It is planned to develop multivariate models in the future by incorporating related properties such as temperature, wind speed, and humidity into the input properties. In addition, it is predicted that metaheuristic

approaches can be used in determining the parameters of the forecasting model.

CONFLICTS OF INTEREST

The authors declare that they have no conflicts of interest.

REFERENCES

- [1] R. K. Sahu, B. Shaw, J. R. Nayak, and Shashikant, "Short/medium term solar power forecasting of Chhattisgarh state of India using modified TLBO optimized ELM", *Engineering Science and Technology, an International Journal*, vol. 24, no. 5, pp. 1180–1200, 2021. DOI: 10.1016/j.jestch.2021.02.016.
- [2] D. E. H. J. Gernaat, H. S. de Boer, V. Daioglou, S. G. Yalew, C. Müller, and D. P. van Vuuren, "Climate change impacts on renewable energy supply", *Nature Climate Change*, vol. 11, pp. 119–125, 2021. DOI: 10.1038/s41558-020-00949-9.
- [3] M. Melikoglu, "The role of renewables and nuclear energy in Turkey's Vision 2023 energy targets: Economic and technical scrutiny", *Renewable and Sustainable Energy Reviews*, vol. 62, pp. 1–12, 2016. DOI: 10.1016/j.rser.2016.04.029.
- [4] S. Das, "Short term forecasting of solar radiation and power output of 89.6 kwp solar PV power plant", *Materials Today: Proceedings*, vol. 39, no. 5, pp. 1959–1969, 2021. DOI: 10.1016/j.matpr.2020.08.449.
- [5] T. Paterova and M. Prauzek, "Estimating harvestable solar energy from atmospheric pressure using deep learning", *Elektronika ir Elektrotechnika*, vol. 27, no. 5, pp. 18–25, 2021. DOI: 10.5755/j02.eie.28874.
- [6] J. Shi, W.-J. Lee, Y. Liu, Y. Yang, and P. Wang, "Forecasting power output of photovoltaic systems based on weather classification and support vector machines", *IEEE Transactions on Industry Applications*, vol. 48, no. 3, pp. 1064–1069, 2012. DOI: 10.1109/TIA.2012.2190816.
- [7] J. Zeng and W. Qiao, "Short-term solar power prediction using a support vector machine", *Renewable Energy*, vol. 52, pp. 118–127, 2013. DOI: 10.1016/j.renene.2012.10.009.
- [8] S. Al-Dahidi, O. Ayadi, J. Adeeb, M. Alrbai, and B. R. Qawasmeh, "Extreme learning machines for solar photovoltaic power predictions", *Energies*, vol. 11, no. 10, p. 2725, 2018. DOI: 10.3390/en11102725.
- [9] M. K. Behera, I. Majumder, and N. Nayak, "Solar photovoltaic power forecasting using optimized modified extreme learning machine technique", *Engineering Science and Technology, an International Journal*, vol. 21, no. 3, pp. 428–438, 2018. DOI: 10.1016/j.jestch.2018.04.013.
- [10] M. Pierro *et al.*, "Data-driven upscaling methods for regional photovoltaic power estimation and forecast using satellite and numerical weather prediction data", *Solar Energy*, vol. 158, pp. 1026–1038, 2017. DOI: 10.1016/j.solener.2017.09.068.
- [11] S. Leva, A. Dolara, F. Grimaccia, M. Mussetta, and E. Ogliari, "Analysis and validation of 24 hours ahead neural network forecasting of photovoltaic output power", *Mathematics and Computers in Simulation*, vol. 131, pp. 88–100, 2017. DOI: 10.1016/j.matcom.2015.05.010.
- [12] C.-M. Huang, S.-J. Chen, S.-P. Yang, and C.-J. Kuo, "One-day-ahead hourly forecasting for photovoltaic power generation using an intelligent method with weather-based forecasting models", *IET Generation, Transmission & Distribution*, vol. 9, no. 14, pp. 1874–1882, 2015. DOI: 10.1049/iet-gtd.2015.0175.
- [13] Z. Yang, M. Mourshed, K. Liu, X. Xu, and S. Feng, "A novel competitive swarm optimized RBF neural network model for short-term solar power generation forecasting", *Neurocomputing*, vol. 397, pp. 415–421, 2020. DOI: 10.1016/j.neucom.2019.09.110.
- [14] A. T. Eseye, J. Zhang, and D. Zheng, "Short-term photovoltaic solar power forecasting using a hybrid Wavelet-PSO-SVM model based on SCADA and Meteorological information", *Renewable Energy*, vol. 118, pp. 357–367, 2018. DOI: 10.1016/j.renene.2017.11.011.
- [15] W. VanDeventer *et al.*, "Short-term PV power forecasting using hybrid GASVM technique", *Renewable Energy*, vol. 140, pp. 367–379, 2019. DOI: 10.1016/j.renene.2019.02.087.
- [16] H. Lin, Q. Sun, and S.-Q. Chen, "Reducing exchange rate risks in international trade: A hybrid forecasting approach of CEEMDAN and multilayer LSTM", *Sustainability*, vol. 12, no. 6, p. 2451, 2020. DOI: 10.3390/su12062451.
- [17] V. Kushwaha and N. M. Pindoriya, "A SARIMA-RVFL hybrid model assisted by wavelet decomposition for very short-term solar PV power generation forecast", *Renewable Energy*, vol. 140, pp. 124–139, 2019. DOI: 10.1016/j.renene.2019.03.020.
- [18] E. Dokur, "Swarm decomposition technique based hybrid model for very short-term solar PV power generation forecast", *Elektronika ir Elektrotechnika*, vol. 26, no. 3, pp. 79–83, 2020. DOI: 10.5755/j01.eie.26.3.25898.
- [19] S. Monjoly, M. André, R. Calif, and T. Soubdhan, "Hourly forecasting of global solar radiation based on multiscale decomposition methods: A hybrid approach", *Energy*, vol. 119, pp. 288–298, 2017. DOI: 10.1016/j.energy.2016.11.061.
- [20] Y. Lin, Y. Yan, J. Xu, Y. Liao, and F. Ma, "Forecasting stock index price using the CEEMDAN-LSTM model", *The North American Journal of Economics and Finance*, vol. 57, art. 101421, 2021. DOI: 10.1016/j.najef.2021.101421.
- [21] Z. Liu, D. Peng, M. J. Zuo, J. Xia, and Y. Qin, "Improved Hilbert–Huang transform with soft sifting stopping criterion and its application to fault diagnosis of wheelset bearings", *ISA Transactions*, vol. 125, pp. 426–444, 2022. DOI: 10.1016/j.isatra.2021.07.011.
- [22] E. Dokur, N. Erdogan, M. E. Salari, C. Karakuzu, and J. Murphy, "Offshore wind speed short-term forecasting based on a hybrid method: Swarm decomposition and meta-extreme learning machine", *Energy*, vol. 248, art. 123595, 2022. DOI: 10.1016/j.energy.2022.123595.
- [23] M. K. Osman, M. Y. Mashor, and H. Jaafar, "Detection of tuberculosis bacilli in tissue slide images using HMLP network trained by extreme learning machine", *Elektronika ir Elektrotechnika*, vol. 120, no. 4, pp. 69–74, 2012. DOI: 10.5755/j01.eie.120.4.1456.
- [24] C. Zhou, K. Yin, Y. Cao, E. Intrieri, B. Ahmed, and F. Catani, "Displacement prediction of step-like landslide by applying a novel kernel extreme learning machine method", *Landslides*, vol. 15, pp. 2211–2225, 2018. DOI: 10.1007/s10346-018-1022-0.
- [25] G.-B. Huang, "An insight into extreme learning machines: Random neurons, random features and kernels", *Cognitive Computation*, vol. 6, pp. 376–390, 2014. DOI: 10.1007/s12559-014-9255-2.
- [26] A. Thangavel and V. Govindaraj, "Forecasting energy demand using conditional random field and convolution neural network", *Elektronika ir Elektrotechnika*, vol. 28, no. 5, pp. 12–22, 2022. DOI: 10.5755/j02.eie.30740.
- [27] G. K. Apostolidis and L. J. Hadjileontiadis, "Swarm decomposition: A novel signal analysis using swarm intelligence", *Signal Processing*, vol. 132, pp. 40–50, 2017. DOI: 10.1016/j.sigpro.2016.09.004.



This article is an open access article distributed under the terms and conditions of the Creative Commons Attribution 4.0 (CC BY 4.0) license (<http://creativecommons.org/licenses/by/4.0/>).